




Cite this: *RSC Adv.*, 2022, 12, 27775

# Photo-enhanced growth of lead halide perovskite crystals and their electro-optical properties†

Shiwei Wang, \*<sup>ab</sup> Yixuan Wang,<sup>a</sup> Qi Wei<sup>a</sup> and Junling Wang \*<sup>c</sup>

Organic–inorganic hybrid perovskites have attracted much attention for opto-electronic applications due to their low trap density, strong light absorption, and superior charge transport performance. Generally, the high efficiency of perovskite electro-optical thin films depends on their high-quality perovskite single crystals. In this work, the external illumination is applied on the perovskite single crystals growing in solution. It was shown that larger size  $\text{CH}_3\text{NH}_3\text{PbI}_3$  single crystals can be obtained under illumination conditions. In addition,  $\text{CH}_3\text{NH}_3\text{PbI}_3$  films are prepared by a one-step spin coating process under illumination, the crystal size and film quality of which have been obviously improved due to the effect of illumination in the film forming process. The efficiency of the average cells based on  $\text{CH}_3\text{NH}_3\text{PbI}_3$  films increased from 15.2% for the normal conditions to 17.7% for the illumination one, which is consistent with the light enhanced growth of  $\text{CH}_3\text{NH}_3\text{PbI}_3$  single crystals in their solution. The “photo-inhibition nucleation” mechanism is proposed to explain the light-induced enhancement of perovskite crystal growth.

Received 8th August 2022  
Accepted 17th September 2022

DOI: 10.1039/d2ra04919h

rsc.li/rsc-advances

## 1. Introduction

Organic–inorganic hybrid perovskites (OIHP) have attracted much attention for solar cells and optoelectronic applications due to their low trap density, strong light absorption, and superior charge transport performance.<sup>1–4</sup> The photoelectric conversion efficiency (PCE) of OIHP-based solar cells has reached more than 24.2% quickly after a short period of development.<sup>5</sup> Several methods have been used to improve the performance of perovskite solar cells, such as synthesis of novel electronic transmission materials,<sup>6,7</sup> hole transport materials,<sup>8</sup> different types of perovskite materials and device structures.<sup>9</sup> However, the type and quality of perovskite crystals is the fundamental source of high efficiency photovoltaic cells.<sup>10</sup> So, the growth of perovskite crystals and their development of electro-optic applications have always been an important subject.<sup>11</sup> Certainly, it is one of the important ways to improve the PCE of perovskite solar cells by improving the quality of perovskite polycrystalline thin films.<sup>12</sup>

The relationship between light, perovskite material, and device performance is a key topic that researchers pay close attention to.<sup>13–15</sup> They have always focused on the research of the response characteristics of the device to light.<sup>16</sup> The light response during

single crystal growth is seldom noticed. Methylazanium iodide perovskite ( $\text{MAPbI}_3$ ) materials have been widely studied in solar cells due to its light absorption and band gap properties, and the study of its physical properties and growth process is often carried out as a typical representative of OIHP materials.<sup>17,18</sup>

In this work,  $\text{MAPbI}_3$  single crystals are prepared by solution precipitation. During single crystal growth, a white light source is applied to light from outside. During the growth of perovskite single crystals in solution, it is found that continuous external light can promote the growth of large-sized single crystals. On this basis,  $\text{MAPbI}_3$  films are prepared by one-step spin coating process under illumination, the crystal size and film quality of which have been obviously improved because of illumination in the film forming process. Therefore, the photoelectrical properties of  $\text{MAPbI}_3$  single crystals and films grown under light conditions are greatly improved.

## 2. Method

### 2.1 Preparation of $\text{MAPbI}_3$ single crystals

$\text{PbI}_2$  (5.5 g, 99.99%, Sigma-Aldrich) and  $\text{CH}_3\text{NH}_3\text{I}$  (2.0 g, 99.9%, Sigma-Aldrich) was mixed in  $\gamma$ -butyrolactone (GBL, 10.0 mL, AR  $\geq 99\%$ , Sigma-Aldrich), then the growth solution would be achieved by sealing the mixed solution in a glass bottle with stirring at 60 °C for 1 h under dark. The glass bottle with a growth solution was left in the oven at 100 °C under illumination for a certain time. All the operations were carried out under dark condition except the special light source used in the experiment.  $\text{MAPbI}_3$  single crystals with different sizes can be obtained by controlling the light intensity and illumination time on the precursor solution.

<sup>a</sup>School of Chemical Engineering, Advanced Research Institute of Materials Science, Changchun University of Technology, Changchun, 130012, China. E-mail: wswjldx2004@163.com

<sup>b</sup>Hainan Vocational University of Science and Technology, Haikou, 571126, China

<sup>c</sup>School of Physics, Southern University of Science and Technology, Shenzhen, 518055, China. E-mail: jwang@sustech.edu.cn

† Electronic supplementary information (ESI) available. See <https://doi.org/10.1039/d2ra04919h>



## 2.2 Device fabrication

To study the dependence of the device performance on illumination conditions, the perovskite absorbing layer was prepared under illumination with different intensity in nitrogen-filled glove box (40% of MAPbI<sub>3</sub> in GBL) by spin coating at 5000 rpm for at least 60 s, chlorobenzene was added after 30 seconds. Then annealed at 100 °C for 1 hour. (Note that perovskite layer remains in the light during spin-coating and annealing). Spiro-OMeTAD/chlorobenzene (72.3 mg mL<sup>-1</sup>) solution was employed with the addition of 17.5 μL of Li-TFSI/acetonitrile (520 mg mL<sup>-1</sup>), and 28.8 μL of 4-*tert*-butyl pyridine. 30 μL of Spiro-OMeTAD solution mixed above was spin-coated on the perovskite film at 3000 rpm for 30 s, where finally, a gold layer with a thickness of 100 nm was deposited as the counter electrode on the top of Spiro-OMeTAD layer through shadow masks *via* thermal evaporation under high vacuum ( $5 \times 10^{-5}$  Torr). The perovskite single crystal device can be obtained by evaporating gold electrode on the larger plane of the perovskite crystal.

## 2.3 Measurements

Keithley 2400 source meter was used to record the photocurrent response signal under 20 V bias voltage with a light intensity of 100 mW cm<sup>-2</sup>. The spectral photo response measurements were performed with a 150 W halogen lamp equipped with a manual monochromator. Optical power meter (SM206-SOLAR solar power meter) was used to measure the incident powers. *J-V* curves of the PSCs were measured using a Keithley 2400 source meter under ambient conditions at room temperature. The light source was a 450 W xenon lamp (Oriel solar simulator) with a Schott K113 Tempax sunlight filter (Prazisions Glas & Optik GmbH) to match AM1.5G. The light intensity was 100 mW cm<sup>-2</sup> calibrated by an NREL-traceable KG5-filtered silicon reference cell. All measurements were taken at room temperature. UV-vis absorption spectra were recorded using Agilent Cary 5000 at room temperature in the absorption mode and the fluorescence spectra were obtained using the PerkinElmer LS55 fluorescence spectrometer with the excitation wavelength of 365 nm. To reduce the sample variance, at least three samples were determined for each group and the average of all spectra presented. X-ray diffraction data were collected on a high-resolution diffractometer by Rigaku Smart lab (Cu-Kα radiation). SEM measurements were carried out in a scanning electron microscope (JSM-7610Fplus, JEOL).

## 3. Results and discussion

MAPbI<sub>3</sub> single crystals are grown from their precursor solutions by the inverse temperature crystallization method at 100 °C, both in dark and under light illumination.<sup>19,20</sup> The differences in crystal size and number can be obviously observed in the eye for the MAPbI<sub>3</sub> single crystals grown with and without illumination. As shown in Fig. 1a, under illumination condition, MAPbI<sub>3</sub> single crystals with small quantity but large size are obtained in the solution. However, the number of MAPbI<sub>3</sub> single crystals grown in the dark is large but the size is small.

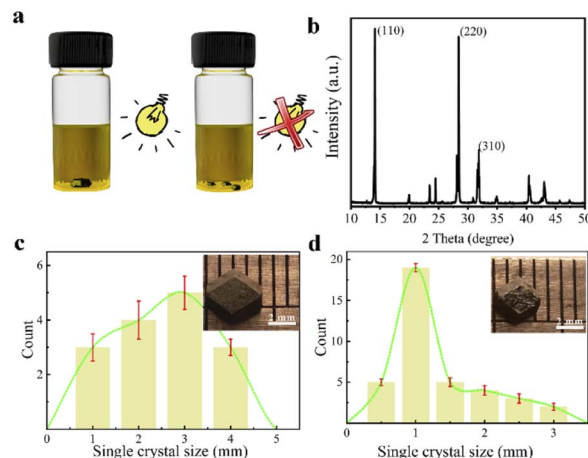


Fig. 1 (a) Growth processes of MAPbI<sub>3</sub> crystals under light and dark conditions, the light intensity of which is 64 mW cm<sup>-2</sup>. (b) XRD curves for MAPbI<sub>3</sub> single crystal. And the statistical data of the size and number of MAPbI<sub>3</sub> single crystals in their precursor solutions under light (c) and dark (d) conditions, respectively. The insert images are the MAPbI<sub>3</sub> single crystal grown from its precursor solution after 36 h.

Besides, different intensities of light are used to grow their single crystals, which can be found that the largest size for MAPbI<sub>3</sub> single crystals were got under the light intensity of 62 mW cm<sup>-2</sup> (Fig. S1†). The structure of MAPbI<sub>3</sub> crystals was characterized by X-ray diffraction (XRD), which characteristic peaks are in good agreement with literature reported (Fig. 1b and S2†).<sup>20,21</sup> It can be confirmed that the structure of perovskite single crystal is not affected by light exposure during growth. By comparing the growth of MAPbI<sub>3</sub> single crystals under light (62 mW cm<sup>-2</sup>) and in dark, as shown in Fig. 1c and d, it is clearly seen from the statistical results that the number of crystals obtained under illumination is less than that in dark. However, the size of the crystals is obvious larger.

In order to exclude the effect of temperature change due to illumination on the growth of MAPbI<sub>3</sub> single crystals, infrared thermometer has been used to track the temperature of the precursor solution. The results show that the temperature fluctuation is less than 0.3 °C, regardless of whether it is in dark or under light (Fig. S3†). It is unlikely that such a small change in the precursor solution temperature will have such a large effect on the growth of MAPbI<sub>3</sub> single crystals.

The photo-inhibition of nucleation theory was proposed to explain the perovskite crystals enhanced grown under illumination. UV-vis absorbance spectrum of MAPbI<sub>3</sub> precursor solutions has been detected to investigate the crystal grown process. As shown in Fig. 2a–c, there are a large number of complexes in the MAPbI<sub>3</sub> precursor solution, such as PbI<sub>4</sub><sup>2-</sup> and PbI<sub>3</sub><sup>-</sup>.<sup>22</sup> With the solution temperature increasing, the lead halide complexes are dissolved due to the H<sup>+</sup> produced from butyrolactone. Then, MAPbI<sub>3</sub> crystal nucleus will precipitate due to more free ions formed from the super-saturation of PbI<sub>n</sub><sup>(n-2)-</sup> complexes in solutions.<sup>23,24</sup> As shown in Fig. 2a and b, the absorption peaks at 325 nm and 375 nm are attributed to PbI<sub>4</sub><sup>2-</sup> and PbI<sub>3</sub><sup>-</sup> complexes in the solution, respectively.<sup>22,25,26</sup> The strength of these absorption peaks are decreased with the



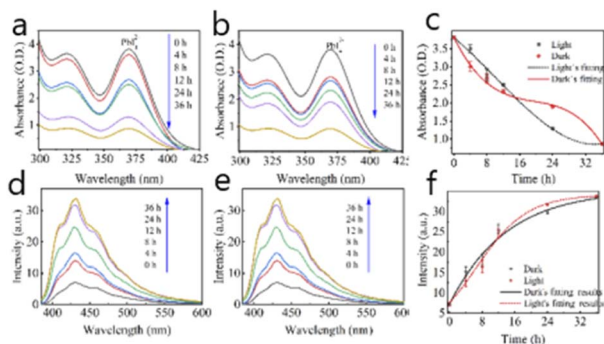


Fig. 2 (a and b) UV-vis spectra of MAPbI<sub>3</sub> precursor solutions with different single crystal growth times under light and dark conditions, respectively. (c) Fitted curves of the absorbance peak at 375 nm. PL spectra of MAPbI<sub>3</sub> precursor solution with different growth times of single crystals under light (d) and dark (e) conditions. (f) Fit curves of the photoluminescence peak at 431 nm.

increase of the growth time. However, the absorption peaks decrease more significantly in the initial stage of crystal growth in dark than those under illumination (Fig. 2c). It suggests that the nucleus is easier to be formed when perovskite single crystal's growth is carried out in dark conditions. So more MAPbI<sub>3</sub> nucleus are precipitated from the solution in dark, which are used to grow for MAPbI<sub>3</sub> single crystals. On the contrary, less MAPbI<sub>3</sub> nucleus are precipitated from the solution under illumination, so the number of MAPbI<sub>3</sub> crystals grown in dark is obviously larger than the ones under light. PbI<sub>n</sub><sup>(n-2)-</sup> colloids in the solution will gradually break down into free ions for the growth of MAPbI<sub>3</sub> single crystals. In the same initial precursor solution, the size of MAPbI<sub>3</sub> single crystals will be larger under illumination than the one under dark due to more free ions in the solution. Note that there is a certain limit to the formation and decomposition of PbI<sub>n</sub><sup>(n-2)-</sup> colloids, that is, the photoinhibition nucleation effect is also within a certain limit, not infinite, therefore, the appropriate light intensity (64 mW cm<sup>-2</sup>) can grow the largest single crystal.

The fluorescence spectrum of precursor solutions is also used to confirm the "photo-inhibition nucleation theory" further. It can be seen from Fig. 2d–f that the intensity of the photoluminescence peak is increasing with the increase of the growing time of MAPbI<sub>3</sub> single crystals, which is attributed to the decrease of iodine ions in solution.<sup>27</sup> The fluorescence characteristic here is attributed to the iodine ion in the solution, which is dissociated from a variety of lead iodide colloids, so it is a trend towards relative equilibrium. However, the increase of absorption peak under dark conditions is more obvious, which shows that the amount of iodine ions in dark is less than the one in light conditions (at least 0–14 h). While the crystal in the solution is just at the nucleation stage, so it can be inferred that light can inhibit the nucleation process of MAPbI<sub>3</sub> crystal by affecting the decomposition of PbI<sub>n</sub><sup>(n-2)-</sup> complexes in the solution. So "photo-inhibition nucleation theory" is proposed to explain the phenomenon of light-induced single crystal growth.

Perovskite films are formed from the process of single crystal precipitation and solvent volatilization. Polycrystals in

perovskite films are also formed by nucleation and growth processes, which is similar to the process of saturated precipitation of perovskite single crystals. The photo-enhanced perovskite single crystal may be suitable for perovskite polycrystalline thin films. According to the "photo-inhibition nucleation theory" for the growth of MAPbI<sub>3</sub> crystals proposed above, MAPbI<sub>3</sub> films have been prepared by one-step spin coating process under illumination and their solar cells based on them was also constructed. As shown in Fig. 3, the average size of MAPbI<sub>3</sub> crystals in the thin films can be obviously observed from the SEM photos of the thin films prepared under dark and light. It can be clearly revealed that the grain size of MAPbI<sub>3</sub> in the film obtained under illumination of 62 mW cm<sup>-2</sup> of white light is obviously larger than that in dark. The statistics of crystal size in thin films are shown in Fig. 3, the laws and

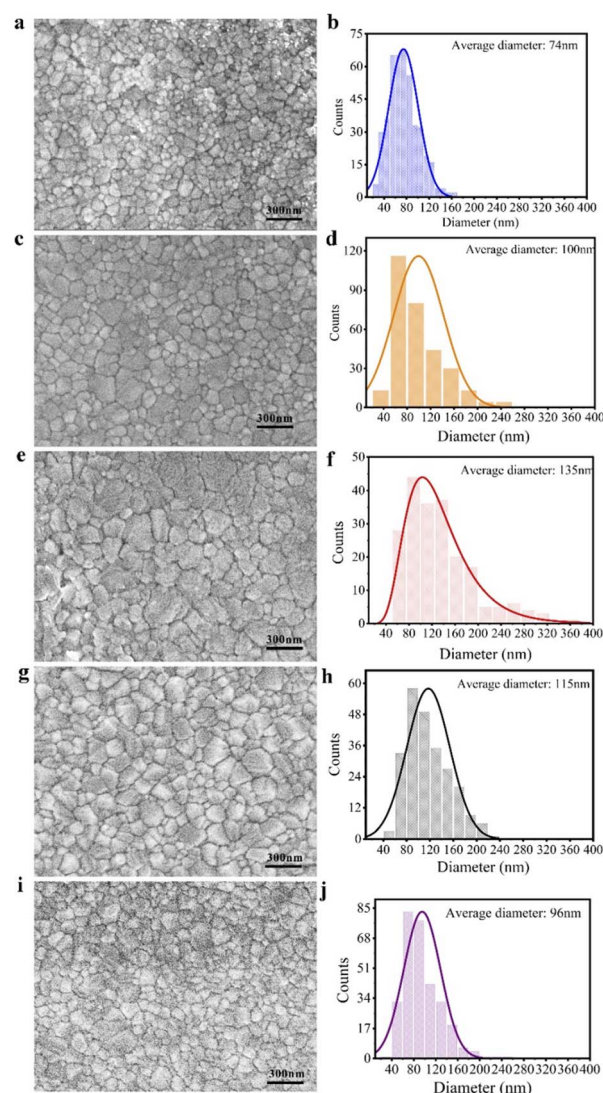


Fig. 3 SEM images of MAPbI<sub>3</sub> films obtained by spin-coating under different illumination intensities ((a) 0 mW cm<sup>-2</sup>, (c) 52 mW cm<sup>-2</sup>, (e) 52 mW cm<sup>-2</sup>, (g) 82 mW cm<sup>-2</sup>, (i) 132 mW cm<sup>-2</sup>). The statistics of the grain diameter distribution of the MAPbI<sub>3</sub> microcrystalline in films ((b, d, f, h and j) is corresponding to the sample of (a, c, e, g and i), respectively).





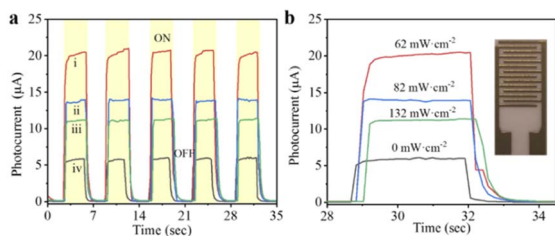


Fig. 4 (a) Photoelectric response for MAPbI<sub>3</sub> films fabricated on interdigital electrode under illumination (1 sun of light intensity and the electrode spacing is 0.14 mm); (b) the enlarged curves for (a) and the intensity of illumination for MAPbI<sub>3</sub> films constructed have been signed-in the curves.

trends of which are exactly the same as that for MAPbI<sub>3</sub> single crystal growth.

Besides, MAPbI<sub>3</sub> polycrystalline films are prepared by one-step spin-coating on the interdigital electrodes under illumination. As shown in Fig. 4, a large photocurrent can be detected when a beam of light illuminates on the surface of the film. In addition, when the light with the intensity of 62 mW cm<sup>-2</sup> is introduced during the film spin-coating process, the obtained MAPbI<sub>3</sub> film shows the highest current value and on/off ratio, which is attributed to the large crystal size and dense stacking structure in the film.<sup>28</sup> Perovskite devices based on FTO/TiO<sub>2</sub>/MAPbI<sub>3</sub>/Spiro-OMeTAD/Au structure are also constructed, the photoelectric transformation efficiencies of which were detected from their *J*-*V* curves. As shown in Fig. 5, the average PCE of

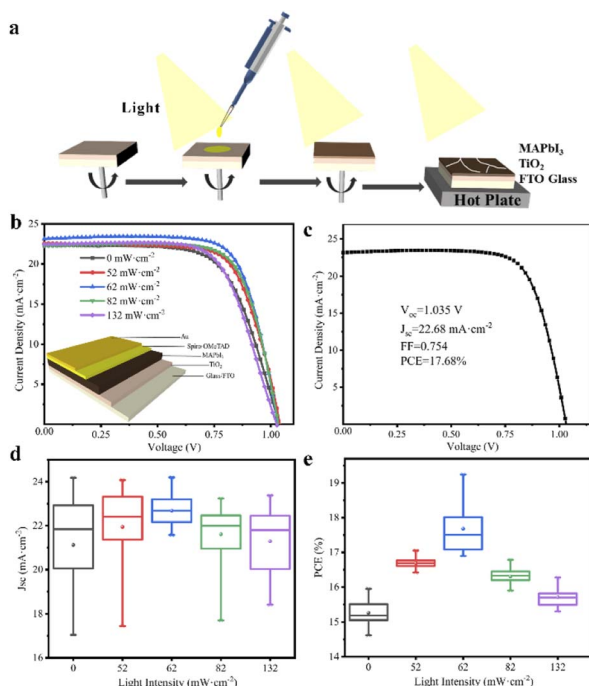


Fig. 5 (a) Scheme for the preparation process of MAPbI<sub>3</sub> films under illumination. (b) *J*-*V* curves for the cells based on MAPbI<sub>3</sub> obtained under different intensities of light, the inset of which is the device structure. (c) *J*-*V* curve and PCE for the cells prepared under illumination with the light intensity of 62 mW cm<sup>-2</sup>. (d and e) Is the statistical data of the *J*<sub>SC</sub> and PCE for the cells (area is 0.09 cm<sup>2</sup>).

the devices is the highest at 17.7%, when their MAPbI<sub>3</sub> films were prepared under the illumination of 62 mW cm<sup>-2</sup> light intensity. It can be confirmed that the high PCE of perovskite device was attributed to its morphology of thin films with compact accumulation of bulk crystals under illumination. In another, it can be observed from Fig. 5c that the short circuit current density (*J*<sub>SC</sub>) of the device is greatly affected by the morphology of MAPbI<sub>3</sub> thin films. When the thin film devices prepared under illumination, not only the value of their *J*<sub>SC</sub> is increased, but also the distribution of *J*<sub>SC</sub> for the 18 devices is more concentrated. In a word, when the perovskite thin film is prepared under illumination, the efficiency of their cells will be higher and the reliability will be better. Through this work, it can be proposed to introduce the illumination into the preparation and production of perovskite thin-film solar cells. It is worth emphasizing that the highest efficiency of perovskite cells is not the goal, but the repeatability of the experimental results of multiple device samples can prove the idea of this work.

In addition, the thermodynamic critical factor in nucleation is the critical free energy of nucleation ( $\Delta G^*$ ) and the critical nucleus size ( $r_k$ ), which can be described with the following (eqn (1) and (2)) (ESI Note 1†):<sup>29–32</sup>

$$\Delta G^* = \frac{\beta_2^3 T_0^2 (2C_0 \alpha_0 - q^2)^2}{54 C_0 \beta_1 Q \times \Delta T} \quad (1)$$

$$r_k = \beta_2 T_0 \frac{2C_0 \alpha_0 - q^2}{3 C_0 \beta_1 Q \times \Delta T} \quad (2)$$

where  $\beta_1$  and  $\beta_2$  are the shape factors used to calculate the volume and surface of crystal nuclei separately,  $Q$  is the latent heat of crystallization,  $\alpha_0$  is the surface tension at zero charge,  $q$  is the charge density,  $C_0$  is the double-layer capacitance,  $T_0$  is the theoretical crystallization temperature, and  $\Delta T$  is the difference between the theoretical crystallization temperature and the actual crystallization temperature.

According to the nucleation kinetics, a stable crystal nucleus can only be formed when their size is larger than the critical nucleus size.<sup>32</sup> According to the “photoinhibition nucleation Theory” and photochemical reaction, there will be less free ions in the solution for the formation of nucleation when the perovskite precursor solution is placed under light.<sup>33–38</sup> At the same time, the migration rate of free ions in solution will be increased due to the effect of light outside.<sup>33–38</sup> So, the charge density on the crystal nucleus surface will be less under the light. According to the equations mentioned above (eqn (1) and (2)), the critical free energy of nucleation ( $\Delta G^*$ ) and the critical nucleus size ( $r_k$ ) will be increased under light ( $\Delta G^*_{\text{light}} > \Delta G^*_{\text{dark}}$  and  $r_{k, \text{light}} > r_{k, \text{dark}}$ ). Thus, the crystal nucleus is more difficult to have existed in stable and grown-up under light than the ones under dark.

After the formation of MAPbI<sub>3</sub> crystal nuclei under light or dark, MAPbI<sub>3</sub> nuclei will continue to grow in the precursor solution to form single crystals. Surprisingly, when other conditions are consistent, the size of MAPbI<sub>3</sub> single crystals grown under light conditions in the solution is obviously larger than the ones under dark, which can be seen from Fig. 1. This was largely due to the vibration frequency of the atom in the



solution will be increased because of appropriate light outside.<sup>39,40</sup> And the driving force of crystal growth under light is larger than under dark ( $\Delta g_{\text{light}} > \Delta g_{\text{dark}}$ ) (it is obtained by eqn (1)). In addition, the electrostatic interaction on the crystal surface caused by the illumination can also accelerate the deposition of free ions and promote the growth of the MAPbI<sub>3</sub> crystals.

## 4. Conclusions

In summary, a photo-enhanced effect on the growth process of MAPbI<sub>3</sub> crystals have been investigated in this work. It can be confirmed that the perovskite crystals can be grown more larger under external illumination. "Photo-inhibition nucleation theory" is proposed preliminarily to explain the dynamic mechanism. It can be inferred that appropriate external illumination can inhibit the formation of perovskite crystal nuclei in the precursor solution but facilitate the growth of the single crystals. The growth law of perovskite single crystal can be directly applied in the preparation process of their thin films. So, the photo responses for MAPbI<sub>3</sub> films constructed by one-step spin coating under illumination are obviously enhanced. Depending on the large single crystal size and dense packing film morphology, the efficiency of MAPbI<sub>3</sub> solar cells constructed based on the illumination MAPbI<sub>3</sub> films are obviously improved compared with the normal devices, the reliability of which can be proved through repeated experiments. This work provides a new method for improving the efficiency of perovskite solar cells, and provides a direction for perovskite research.

## Conflicts of interest

There are no conflicts to declare.

## Acknowledgements

The authors gratefully acknowledge the funding of this research by the National Natural Science Foundation of China (Grant no. 21204087); the Changchun Science and Technology Development Plan Project (21ZY39); Jilin Innovation and Entrepreneurship Talent Project (2021Y002); Jilin Science and Technology Development Project (YDZJ202201ZYTS557, 20220508154RC, 20200403142SF and 20210203111SF).

## References

- 1 J. P. Correa-Baena, M. Saliba, T. Buonassisi, M. Gratzel, A. Abate, W. Tress and A. Hagfeldt, Promises and challenges of perovskite solar cells, *Science*, 2017, **358**, 739–744.
- 2 A. K. Jena, A. Kulkarni and T. Miyasaka, Halide Perovskite Photovoltaics: Background, Status, and Future Prospects, *Chem. Rev.*, 2019, **119**, 3036–3103.
- 3 K. Y. Wang, G. C. Xing, Q. H. Song and S. M. Xiao, Micro- and Nanostructured Lead Halide Perovskites: From Materials to Integrations and Devices, *Adv. Mater.*, 2021, **33**, 2000306.
- 4 D. Yang, R. Yang, S. Priya and S. Liu, Recent Advances in Flexible Perovskite Solar Cells: Fabrication and Applications, *Angew. Chem., Int. Ed.*, 2019, **58**, 4466–4483.
- 5 <https://www.nrel.gov/pv/cell-efficiency.html>.
- 6 Y.-Y. Zhou, H. Sternlicht and N. P. Padture, Transmission Electron Microscopy of Halide Perovskite Materials and Devices, *Joule*, 2019, **3**, 641–661.
- 7 S. Ravishankar, S. Gharibzadeh, C. Roldán-Carmona, G. Grancini, Y. Lee and M. Ralaivisoa, Influence of Charge Transport Layers on Open-Circuit Voltage and Hysteresis in Perovskite Solar Cells, *Joule*, 2018, **2**, 788–798.
- 8 G. W. Kim, H. Choi, M. Kim, J. Lee, S. Y. Son and T. Park, Hole Transport Materials in Conventional Structural (n-i-p) Perovskite Solar Cells: From Past to the Future, *Adv. Energy Mater.*, 2020, **10**, 1903403.
- 9 P. Schulz, D. Cahen and A. Kahn, Halide Perovskites: Is It All about the Interfaces?, *Chem. Rev.*, 2019, **119**, 3349–3417.
- 10 J. W. Lee, D. K. Lee, D. N. Jeong and N. G. Park, Control of Crystal Growth toward Scalable Fabrication of Perovskite Solar Cells, *Adv. Funct. Mater.*, 2019, **29**, 1807047.
- 11 C. Liu, Y.-B. Cheng and Z.-Y. Ge, Understanding of perovskite crystal growth and film formation in scalable deposition processes, *Chem. Soc. Rev.*, 2020, **49**, 1653–1687.
- 12 M. A. Haque, J. Troughton and D. Baran, Processing-Performance Evolution of Perovskite Solar Cells: From Large Grain Polycrystalline Films to Single Crystals, *Adv. Energy Mater.*, 2020, **10**, 1902762.
- 13 H.-Q. Cao, J.-Z. Li, Z. Dong, J. Su, J.-J. Chang, Q. Zhao, Z.-Y. Li, L.-Y. Yang and S.-G. Yin, Reducing Defects in Perovskite Solar Cells with White Light Illumination-Assisted Synthesis, *ACS Energy Lett.*, 2019, **4**, 2821–2829.
- 14 W. Tress, K. Domanski, B. Carlsen, A. Agarwalla, E. A. Alharbi, M. Graetzel and A. Hagfeldt, Performance of perovskite solar cells under simulated temperature-illumination real-world operating conditions, *Nat. Energy*, 2019, **4**, 568–574.
- 15 F. Zheng, W.-J. Chen, T.-L. Bu, K. P. Ghiggino, F.-Z. Huang, Y.-B. Cheng, P. Tapping, T. W. Kee, B.-H. Jia and X.-M. Wen, Triggering the Passivation Effect of Potassium Doping in Mixed-Cation Mixed-Halide Perovskite by Light Illumination, *Adv. Energy Mater.*, 2019, **9**, 1901016.
- 16 Y.-B. Yuan and J.-S. Huang, Ion Migration in Organometal Trihalide Perovskite and Its Impact on Photovoltaic Efficiency and Stability, *Acc. Chem. Res.*, 2016, **49**, 286–293.
- 17 J. Haruyama, K. Sodeyama, L. Y. Han and Y. Tateyama, Surface Properties of CH<sub>3</sub>NH<sub>3</sub>PbI<sub>3</sub> for Perovskite Solar Cells, *Acc. Chem. Res.*, 2016, **49**, 554–561.
- 18 S.-N. Yun, X. Zhou, J. Even and A. Hagfeldt, Theoretical Treatment of CH<sub>3</sub>NH<sub>3</sub>PbI<sub>3</sub> Perovskite Solar Cells, *Angew. Chem., Int. Ed.*, 2017, **56**(18), 15806–15817.
- 19 B. Li, Y. Kawakita, Y. Liu, M. Wang, M. Matsuura and K. Shibata, Polar Rotor Scattering as Atomic-level Origin of Low Mobility and Thermal Conductivity of Perovskite CH<sub>3</sub>NH<sub>3</sub>PbI<sub>3</sub>, *Nat. Commun.*, 2017, **8**, 16086.
- 20 Y. Zhou, L. You, S.-W. Wang, Z.-L. Ku, H.-J. Fan and J.-L. Wang, Giant Photostriction in Organic-Inorganic Lead Halide Perovskites, *Nat. Commun.*, 2016, **7**, 11193.



- 21 Y.-C. Liu, Z. Yang, D. Cui, X.-D. Ren, J.-K. Sun, X.-J. Liu, J.-R. Zhang, Q.-B. Wei, H.-B. Fan, F.-Y. Yu, X. Zhang, C.-M. Zhao and S.-Z. Liu, Two-Inch-Sized Perovskite  $\text{CH}_3\text{NH}_3\text{PbX}_3$  ( $\text{X} = \text{Cl}, \text{Br}, \text{I}$ ) Crystals: Growth and Characterization, *Adv. Mater.*, 2015, **27**, 5176–5183.
- 22 B.-C. Li, F. H. Isikgor, H. Coskun and J. Y. Ouyang, The Effect of Methylammonium Iodide on the Supersaturation and Interfacial Energy of the Crystallization of Methylammonium Lead Triiodide Single Crystals, *Angew. Chem., Int. Ed.*, 2017, **56**, 16073–16076.
- 23 J. W. Lee, D. J. Seol, A. N. Cho and N. G. Park, High-Efficiency Perovskite Solar Cells Based on the Black Polymorph of  $\text{HC}(\text{NH}_2)_2\text{PbI}_3$ , *Adv. Mater.*, 2014, **26**, 4991–4998.
- 24 F. Zheng, H. Takenaka, F.-G. Wang, N. Z. Koocher and A. M. Rappe, First-Principles Calculation of the Bulk Photovoltaic Effect in  $\text{CH}_3\text{NH}_3\text{PbI}_3$  and  $\text{CH}_3\text{NH}_3\text{PbI}_{3-x}\text{Cl}_x$ , *J. Phys. Chem. Lett.*, 2015, **6**, 31–37.
- 25 D.-Q. Bi, L. Yang, G. Boschloo, A. Hagfeldt and E. M. J. Johansson, Effect of Different Hole Transport Materials on Recombination in  $\text{CH}_3\text{NH}_3\text{PbI}_3$  Perovskite-Sensitized Mesoscopic Solar Cells, *J. Phys. Chem. Lett.*, 2013, **4**, 1532–1536.
- 26 M. Shirayama, H. Kadowaki, T. Miyadera, T. Sugita, M. Kato and M. Tamakoshi, Optical Transitions in Hybrid Perovskite Solar Cells: Ellipsometry, Density Functional Theory, and Quantum Efficiency Analyses for  $\text{CH}_3\text{NH}_3\text{PbI}_3$ , *Phys. Rev. Appl.*, 2016, **5**, 014012.
- 27 L. Ma, F. Hao, C. C. Stoumpos, B. T. Phelan, M. R. Wasielewski and M. G. Kanatzidis, Carrier Diffusion Lengths of over 500 nm in Lead-Free Perovskite  $\text{CH}_3\text{NH}_3\text{SnI}_3$  Films, *J. Am. Chem. Soc.*, 2016, **138**, 14750–14755.
- 28 W.-Y. Nie, H. Tsai, R. Asadpour, J. C. Blancon, A. J. Neukirch, G. Gupta, J. J. Crochet, M. Chhowalla, S. Tretiak, M. A. Alam, H. L. Wang and A. D. Mohite, High-efficiency solution-processed perovskite solar cells with millimeter-scale grains, *Science*, 2015, **347**, 522–525.
- 29 G. D. Botsaris, in *Industrial Crystallization*, ed. J. W. Mullin, Springer, Boston, 1975.
- 30 P. W. V. Lorenz Ratke, *Growth and Coarsening: Ostwald Ripening in Material Processing*, Springer, 2002.
- 31 W. Li, M. U. Rothmann, A. Liu, Z.-Y. Wang, Y.-P. Zhang, A. R. Pascoe, J. F. Lu, L.-C. Jiang, Y. Chen, F.-Z. Huang, Y. Peng, Q.-L. Bao, J. Etheridge, U. Bach and Y. B. Cheng, Phase Segregation Enhanced Ion Movement in Efficient Inorganic  $\text{CsPbIBr}_3$  Solar Cells, *Adv. Energy Mater.*, 2017, **7**, 1700946.
- 32 A. Ummadisingu, L. Steier, J. Y. Seo, T. Matsui, A. Abate, W. Tress and M. Grätzel, The Effect of Illumination on The Formation of Metal Halide Perovskite Films, *Nature*, 2017, **545**, 208–212.
- 33 R. Murai, H. Y. Yoshikawa, Y. Takahashi and M. Maruyama, Enhancement of Femtosecond Laser-induced Nucleation of Protein in a Gel Solution, *Appl. Phys. Lett.*, 2010, **96**, 3475.
- 34 K. Nakamura, Y. Sora, H. Y. Yoshikawa, Y. Hosokawa, R. Murai and H. Adachi, Femtosecond Laser-induced Crystallization of Protein in Gel Medium, *Appl. Surf. Sci.*, 2007, **253**, 6425–6429.
- 35 G. B. Wu, R. Liang, M. Z. Ge, G. X. Sun, Y. Zhang and G. C. Xing, Surface Passivation Using 2D Perovskites toward Efficient and Stable Perovskite Solar Cells, *Adv. Mater.*, 2021, **33**, 2000306.
- 36 H. Y. Yoshikawa, R. Murai, S. Sugiyama, G. Sasaki, T. Kitatani and Y. Takahashi, Femtosecond Laser-induced Nucleation of Protein in Agarose Gel, *J. Cryst. Growth*, 2009, **311**, 956–959.
- 37 V. Adinolfi, O. Ouellette, M. I. Saidaminov, G. Walters, A. L. Abdelhady and O. M. Bakr, Fast and Sensitive Solution-Processed Visible-Blind Perovskite UV Photodetectors, *Adv. Mater.*, 2016, **28**, 7264–7268.
- 38 X. Li, J. Xu, J.-C. Luan, X.-L. Yu, B. Zhang, S.-Y. Dai and J.-X. Yao, Preparation of  $\text{CH}_3\text{NH}_3\text{PbCl}_3$  film with a large grain size using  $\text{PbI}_2$  as Pb source and its application in photodetector, *Mater. Lett.*, 2018, **220**, 108–111.
- 39 O. Boyarkin, T. R. Rizzo, D. S. Perry, O. Boyarkin, T. R. Rizzo and D. S. Perry, Intramolecular energy transfer in highly vibrationally excited methanol. II. Multiple time scales of energy redistribution, *J. Chem. Phys.*, 1999, **110**, 11346.
- 40 C. Molinaro, S. Marguet, L. Douillard, F. Charra and C. Fiorini-Debuisschert, From plasmon-induced luminescence enhancement in gold nanorods to plasmon-induced luminescence turn-off: a way to control reshaping, *Phys. Chem. Chem. Phys.*, 2018, **20**, 12295–12302.

